

# SWIFTSIN: A High-Resolution Ion Isolation Waveform for the Miniaturized Linear ion Trap Mass Spectrometer by Coarse to Fine Excitation

Xinyue Ding<sup>1</sup>, Quan Yu<sup>1</sup>, Xinqiong Lu<sup>2</sup>, Xiaohao Wang<sup>1</sup>, Xinming Huo<sup>3,\*</sup>, Xiang Qian<sup>1,\*</sup>

1. Shenzhen International Graduate School, Tsinghua University, Shenzhen, 518055, China
2. Shenzhen Chin Instrument Co. Ltd., Shenzhen, 518055, China
3. School of Biomedical Engineering, Shenzhen Campus of Sun Yat-Sen University, Shenzhen, 518107, China

\* Corresponding Author: qian.xiang@sz.tsinghua.edu.cn, huoxm@mail.sysu.edu.cn

**ABSTRACT:** To figure out the reason for the drawback of the SWIFT waveform and realize the high-resolution ion isolation on the miniaturized linear ion trap mass spectrometer, we studied the efficiency that ions can be excited under different excitation periods and amplitudes at different frequencies and compared the overlap rates of the effective excitation bandwidths of the adjacent ions. According to this, we purposed a new coarse-to-fine isolation waveform named SWIFTSIN. By superposing one or more sinusoidal waveforms on the SWIFT waveform and modulating the phases of the superposed sinusoidal waveforms, the generated SWIFTSIN waveform achieved unit mass isolation on the miniaturized linear ion trap mass spectrometer without reducing the intensity of the target ion. The isolation ability of the SWIFTSIN waveform was verified by isolating a single isotope peak in the mixed samples.

With high sensitivity and specificity, mass spectrometry has been widely used and playing an increasingly important role in biological research, food and drug analysis, explosive detection, etc.<sup>1-4</sup> Compared with the large-scale instruments used in the laboratory, the miniaturized ion trap mass spectrometer is more suitable for on-site analysis because of its portability and has attracted more and more researchers' attentions.<sup>5-8</sup> Unfortunately, the reduction of the volume has brought a series of negative effects on instrument performance. For examples, the reduction of the ion trap size limits the capacity of ion storage, intensifies the space charge effect inside; and the reduction of the radio frequency (RF) power supply volume limits the maximum RF voltage. These will ultimately bring negative impacts on the resolution, sensitivity, and ion detection range of the miniaturized ion trap mass spectrometer.<sup>9-12</sup>

Broadband waveform excitation is an important technology that can be applied to improve the analytical performance of the miniaturized ion trap mass spectrometer. The purpose of the technology is to activate the trapped ions selectively, which is also called ion isolation. By trapping and isolating the ion of interest and wiping out all other ions before scanning, the space charge effect can be significantly reduced, the signal-to-noise ratio, the analytical sensitivity, and the quantitative analysis ability of mass spectrometry can be improved.<sup>9, 13, 14</sup> Tandem mass spectrometry is also an important way of mass spectrometry analysis.<sup>15-17</sup> In this mode, a selected specific mass-to-charge ratio ion can be isolated first, and then the target ion

in the trap can be fragmented through collision-induced dissociation to obtain more abundant fragment information of the fragmented precursor ion and improve the accuracy of material identification. In the above process, isolation can simplify the information of the tandem mass spectrum and help to further establish the relationship between the target ion and the productions.<sup>18-20</sup> High-resolution ion isolation tandem mass spectrometry can also be used to predict the molecular formula of the compound and obtain the cracking pathway of the compound; this is an important analysis function mainly set in large-scale mass spectrometers,<sup>21, 22</sup> but seldom reported in miniaturized instruments.

The commonly used broadband waveform excitation technology is the stored waveform inverse Fourier transform (SWIFT) technology,<sup>23-27</sup> others include filtered noise field technology<sup>28, 29</sup> and mixed frequency modulation technology.<sup>30, 31</sup> The common feature of the waveforms generated by these techniques is that they all contain specific frequency components which correspond to the secular frequencies of the ions that shouldn't be isolated, to achieve the selective excitation of the ions with different mass-to-charge ratios. The SWIFT waveform is generated by a specific amplitude spectrum through secondary phase modulation and then by inverse Fourier transform.<sup>32-34</sup> Although the SWIFT waveform is widely used, it also has some disadvantages. When applied to the miniaturized ion trap mass spectrometer, the isolation resolution of the SWIFT waveform is insufficient. Due to the reduction of the overall volume of the miniaturized ion trap mass spectrometer, the amplitude of the RF voltage is also limited and as a consequence, the  $q$  value of the ion operating point is low, which will make the secular frequency interval between the adjacent ions smaller, especially for the ions with high mass-to-charge ratios.<sup>19, 35</sup> Therefore, when an attempt is made to isolate a target ion with a narrow isolation window, the energy of the adjacent frequency components used to excite the other ions may cause the false excitation of the target ion and greatly reduce the intensity.

Many attempts at sequence design have been cited to achieve the high-resolution isolation of the target ion.<sup>18, 35, 36</sup> However, these methods greatly increase the complexity of the analysis sequence or increase the period of the whole analysis sequence, which is detrimental to the on-site detection. Here, we explored the excitation of the ions under different excitation periods and amplitudes at different frequencies and obtained the absorption frequency bandwidths of the ions with different mass-to-charge ratios under these excitation conditions, and then proposed a measurement of effective excitation frequency bandwidth. We found that when the absorption frequency bandwidths of the adjacent ions overlap less, it was easier to achieve high-resolution isolation. Accordingly, a simple yet efficient isolation waveform SWIFTSIN was proposed for the high-resolution isolation of the target ion. The waveform was achieved by superposing one or more sinusoidal waveforms with a specific frequency on the traditional SWIFT waveform and adjusting the phases of the superposed sinusoidal waveforms. The period of each frequency of the sinusoidal waveform was longer than that of each frequency in the SWIFT waveform, but the amplitude was lower, thus achieving a "softer" and "coarse-to-fine" excitation effect. Our results indicated that the unit mass isolation of the target ion was achieved with almost no loss of the target ion intensity. The mass spectrum of the fragmented ions obtained after the isolation of the precursor ion was also been purified. The high-resolution isolation technology applied to the miniaturized ion

trap mass spectrometer is expected to improve the field analytical ability of the miniaturized mass spectrometer.

## EXPERIMENTAL SECTION

**Instrumentation.** Experiments were performed on a custom-made linear ion trap mass spectrometer with a continuous atmospheric pressure interface. The distance between the field center and the surface of the two electrodes was 4 mm and 4.25 mm. The RF voltage and auxiliary AC excitation signal were applied on the two pairs of hyperbolic electrodes, respectively. Using a two-stage vacuum chamber, the first vacuum chamber had a small ion funnel for ion transmission, the RF frequency was 929 kHz. The ion trap was in the second vacuum chamber, the RF frequency was 1227 kHz. A Rotary Vacuum pump RVD-2 (pumping speed 120 L/min, Kyky Technology Co., Ltd, Beijing, China), and an Hipace 80 turbo molecular pump (pumping speed 67 L/s, Pfeiffer Vacuum, Asslar, Germany) were used to extract the vacuum. Finally, the pressure in the second vacuum chamber could be maintained at ~0.12 pa. An entrance lens was placed between the ion trap and the skimmer which was between the two vacuum chambers, and these three lenses together served as an einzel lens. The isolation waveform could be generated by the Matlab program, downloaded to the main control board, and finally converted to the analog signal output by a 14-bit digital-analog converter. In the experiment, the normal scan rate was about 500<sup>Th</sup>/s, and the period of the isolation waveform was 21 ms. For more detail descriptions of the instrumentation, it can be referred to our previous works.<sup>37, 38</sup>

**Chemical Samples.** The chemical samples used in this study included dioxopromethazine hydrochloride, rotundine, rosiglitazone, pioglitazone, and repaglinide. All the samples were purchased from J&K Technology Co., Beijing, China, and were diluted in methanol to final concentrations of ~1mg/L.

**Waveform Calculation.** The SWIFT waveform and the SWIFTSIN waveform were calculated and applied in the isolation experiments. The core idea of the SWIFT waveform design is the inverse Fourier transform. The notch frequency band of the magnitude spectrum is designed according to the secular frequency of the isolated ion, and the phase is modulated according to the quadratic phase modulation algorithm,<sup>39</sup> finally, the isolation waveform is generated by inverse Fourier transform. The magnitude spectrum of the SWIFT waveform is generally conceived as a rectangular amplitude spectrum. Assuming that the amplitude of the rectangular spectrum is  $A_0$ , the corresponding SWIFT waveform is<sup>14, 33</sup>

$$f(t) = \frac{A_0}{2\pi} \int_{-\infty}^{+\infty} e^{jp(\omega)} e^{j\omega t} d\omega, \quad (1)$$

where  $p(\omega)$  is the phase function. The quadratic phase function can be expressed as

$$p(\omega) = -\frac{1}{2} \frac{(\omega - \omega_0)^2 (t_1 - t_0)}{\omega_1 - \omega_0} - t_0 \omega, \quad (2)$$

where  $\omega_0$  to  $\omega_1$  is the frequency range of the SWIFT waveform, and  $t_0$  to  $t_1$  is the time period. Figure 1a plots a SWIFT waveform with a frequency band from 0 kHz to 600 kHz and a notch from 220 kHz to 240 kHz. The period is 21 ms. Figure 1b plots the magnitude spectrum, and Figure 1c plots the time-frequency spectrum. Figure 1d is a SWIFT waveform calculated with the same frequency band, but the energy is mainly concentrated in the first 15 ms. Figure 1e plots the magnitude spectrum, and Figure 1f plots the time-frequency spectrum.

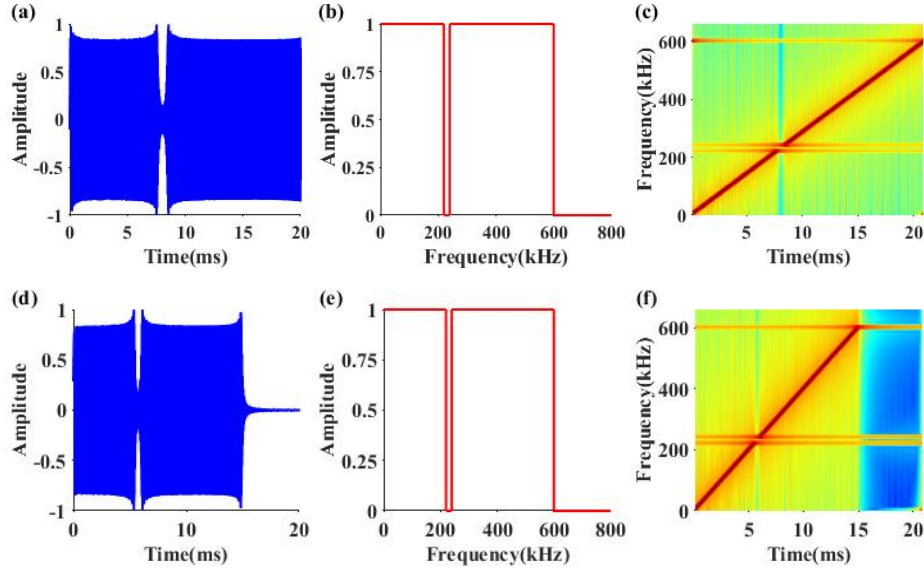


**Figure 1.** (a) SWIFT waveform with a notch from 220 kHz to 240 kHz. (b), (c) The Magnitude spectrum and the time-frequency spectrum of the SWIFT waveform. (d) SWIFT waveform with a notch from 220 kHz to 240 kHz but the energy is mainly concentrated in the first 15 ms of the period. (e), (f) The amplitude and the time-frequency spectrum of the second SWIFT waveform.

To improve the isolation resolution of the isolation waveform, the reason why the SWIFT waveform is difficult to achieve high-resolution isolation without losing the intensity of the isolated target ion was explored and the SWIFTSIN waveform was designed. The SWIFTSIN waveform was constructed by superposing one or more sinusoidal waveforms on the SWIFT waveform. This design aimed to use a large frequency notch SWIFT waveform to achieve coarse isolation, and then use one or more sinusoidal waveforms with specific frequencies to fine excite the other ions near the target ion that were not excited by the coarse isolation. The waveform contracting and superposing operations were used here to avoid an increase in the detection period. To ensure that the ions far away from the target ion were first excited, and to reduce the influence of the space charge effect in the ion trap during the fine isolation, the SWIFT waveform was compressed to the first 15 ms in the time domain like the waveform in Figure 1d. Successively, one or more 5 ms sinusoidal waveforms were superposed and superposed between 15 ms and 20 ms of the SWIFT waveform. The design of the high-resolution isolation waveform didn't use a shorter period of SWIFT waveform splicing sinusoidal waveforms was done to not reduce the resolution of the SWIFT waveform. The following is a design example of a SWIFTSIN waveform. The frequency of the superposed sinusoidal waveform is 229.2 kHz. Figure 2a plots the time domain waveform of a

SWIFTSIN waveform with a large notch from 220 kHz to 240 kHz. Figure 2b plots the magnitude spectrum, and Figure 2c plots the time-frequency spectrum.

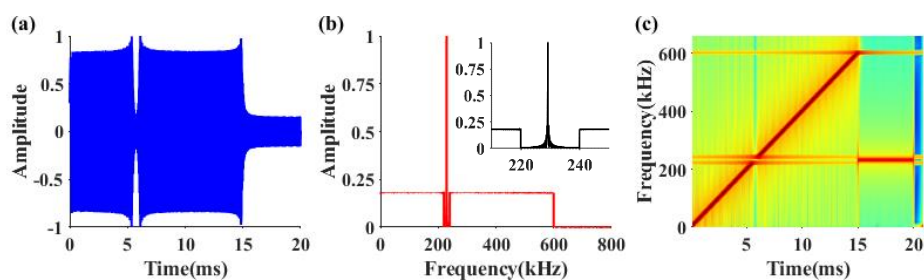


**Figure 2.** SWIFTSIN waveform with a notch from 220 kHz to 240 kHz and superposed a 229.2 kHz sinusoidal waveform. (a) Time domain waveform. (b) Magnitude spectrum. (c) Time-frequency spectrum.

## RESULTS AND DISCUSSIONS

**The SWIFT waveform isolation.** When the isolation waveform is applied to the miniaturized ion trap mass spectrometer and the requirement for the isolation resolution is not high, the SWIFT waveform is usually the ideal choice. However, when the requirement for the isolation resolution is high, the SWIFT waveform will expose some problems, as mentioned above. Here, we tried to isolate the isotope ion (labeled as  $A + 1$ , at 358  $m/z$ ) of pioglitazone (the other isotope ions of it were labeled as  $A$  and  $A + 2$ , at 357  $m/z$  and 359  $m/z$ ) and showed the isolation defect of the SWIFT waveform. The RF voltage at the full scan was  $744 V_0$  to  $930 V_0$ , the frequency of the auxiliary AC was 200 kHz, and its amplitude was  $0.5 V_0$ . Figure 3a plots the mass spectrum of 1 mg/L pioglitazone with an ion injection period of 200 ms. The isolated setting was: RF voltage,  $828 V_0$ , and a SWIFT waveform with a frequency band from 0 kHz to 600 kHz, a notch from 198 kHz to 201 kHz, and a period of 21 ms. To achieve the high-resolution isolation of the  $A+1$  isotope ion, two methods were tried. One was to narrow the notch band. The notch frequency range of the waveform was adjusted to 198 kHz to 199.8 kHz and 198 kHz to 199.6 kHz respectively. Here, we tried to reduce the notch frequency range from one side, that was, we first tried to excite the  $A$  isotope ion without losing the intensity of the  $A + 1$  isotope ion as much as possible. Figure 3b plots the result of the target ion isolation after adjusting the notch frequency range. When the notch frequency range was gradually reduced, The  $A$  isotope ion was gradually excited and the intensity decreased continuously. However, when the intensity of the  $A$  isotope ion remained about 3%, the intensity of the  $A + 1$  isotope ion lost 48%, which could be considered as the false excitation of the  $A + 1$  isotope ion caused by the excitation of the  $A$  isotope ion. The second high-resolution isolation attempt was to increase the frequency amplitude at the notch boundary and change the frequency amplitude at 201kHz on the right side of the notch frequency band to be 30 times and 35 times the original. As can be seen from Figure 3c, with the increase of the frequency amplitude of 201 kHz, the excitation efficiency of the  $A$  isotope ion was increasing. However, a similar situation also occurred, when the intensity of the  $A$  isotope ion remained at about 3%, the intensity of the  $A + 1$  isotope ion lost 33%. It could be suggested that the lack of the high-resolution isolation ability of the SWIFT waveform was

mainly reflected in the error excitation of the isolated target ion, that was when the A isotope ion was excited, the A + 1 isotope ion could also absorb part of the energy and get excited.

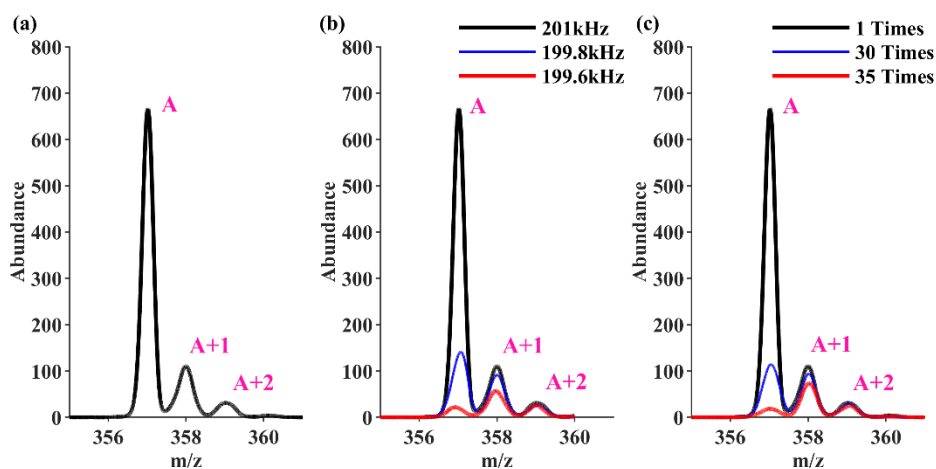


**Figure 3.** Isolation results using the SWIFT waveform, the sample is 1mg/L pioglitazone. (a) Isolation result using the SWIFT waveform with a notch from 198 kHz to 201 kHz. (b) Isolation results using the SWIFT waveform after gradually narrowing the notch band. (c) Isolation results of the SWIFT waveform after changing the edge frequency amplitude of the notch frequency band.

**Effective excitation frequency bandwidth.** To verify the above conjecture, experiments were designed to explore the frequency bandwidths of the ions with different mass-to-charge ratios that could be excited effectively, and the overlap of the effective excitation frequency bandwidths of the ions was investigated. In particular, the exciting process of adding a single sinusoidal waveform before scanning was studied. By changing the frequency, period, and amplitude of the sinusoidal waveform, we could get the efficiencies of the ions that could be excited with the change of these excitation parameters. The sample was still 1 mg/L pioglitazone.

When the frequency of the sinusoidal waveform changed from small to large, the isotope ions A + 2, A + 1, and A were excited respectively. The mass spectrum obtained after the full scan plots, the intensity of the ions after different excitation conditions, and then the excitation efficiencies were obtained. Here we defined effective excitation when the excitation efficiency was greater than or equal to 50 %. Fig. 4a plots the frequency intervals from the A + 2 isotope ion was first effectively excited to the A isotope ion was last effectively excited under different excitation conditions. It could be seen that with the increase of the excitation periods and the excitation amplitudes, the frequency intervals became larger. We suggest that's because the increase in the excitation periods and the excitation amplitudes brought an increase in excitation energy. An increase in the overall frequency interval might imply an increase in the effective excitation bandwidth per mass-to-charge ratio ion and might cause the overlap of the effective excitation frequency bandwidths of the adjacent ions. An extreme case is that the effective excitation frequency bandwidths of the three ions all overlap. It is difficult to attempt to excite only the A isotope ion or the A + 1 isotope ion without affecting the adjacent ions. Figure 4b plots the ratio of the effective excitation frequency bandwidths of the ions with one mass-to-charge ratio (the averages of three mass-to-charge ratio ions) to the

frequency intervals from the A + 2 isotope ion was first effectively excited to the A isotope ion was last effectively excited under different excitation conditions. It can be seen that the overlap of the effective excitation frequency bandwidths of the ions increased with the increasing of the excitation periods and the excitation amplitudes. To effectively excite the adjacent ions without reducing the intensity of the target ion, we should make the effective excitation frequency bandwidths of the adjacent ions overlap as little as possible. Figure 4c plots the excitation efficiencies at different frequencies when the excitation period was 0.1ms and the excitation amplitude was  $3V_0$ . Figure 4d plots the excitation efficiencies of the ions at different frequencies when the excitation period was 5ms and the excitation amplitude was  $0.2 V_0$ . It can be seen that under the second excitation condition, the effective excitation frequency bandwidths of the ions became narrow, and the overlap of the excitation frequency bandwidths of the ions with different mass-to-charge ratios decreased. Using the 198 kHz frequency was expected to realize the excitation of the A + 2 isotope ion without affecting the A + 1 isotope ion. Similarly, using the 199.5 kHz frequency was expected to realize the excitation of the A isotope ion without affecting the A + 1 isotope ion. To achieve high-resolution excitation, the excitation parameters were used in Figure 4d should be referred to in the design of the SWIFTSIN waveform.

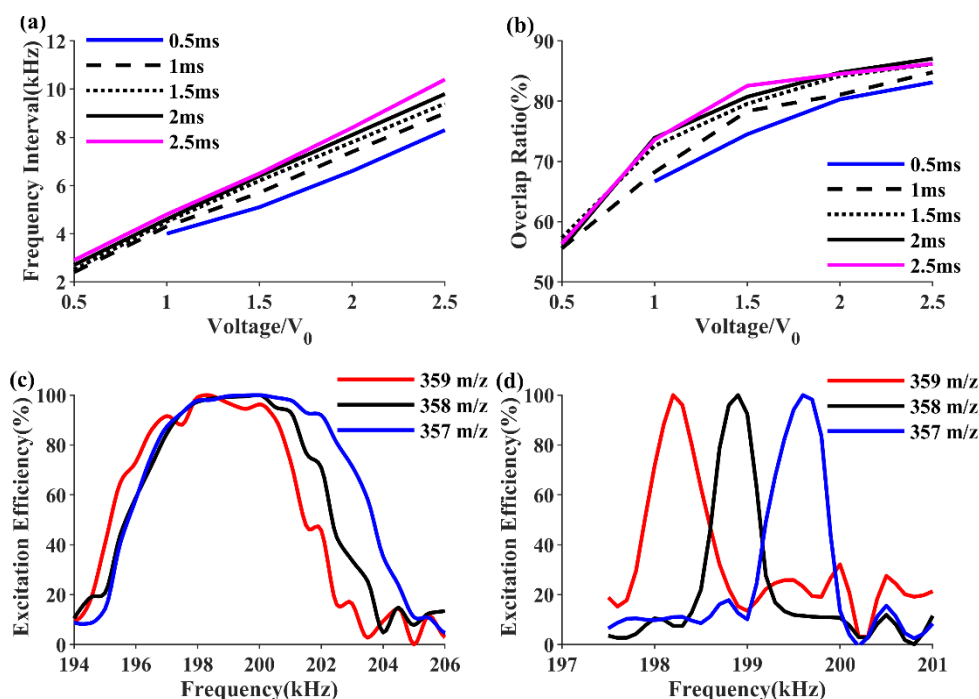


**Figure 4.** Study on the excitation frequency bandwidths of the ions, the sample was 1mg/L pioglitazone (a) The frequency intervals from the A + 2 isotope ion were first effectively excited to the A isotope ion was last effectively excited under different excitation conditions. (b) The ratios of the effective excitation frequency bandwidths of the ions with one mass-to-charge ratio (The average of three mass-to-charge ratio ions) to the frequency intervals. (c) The excitation efficiencies of the ions at different frequencies when the excitation period was 0.1ms and the excitation amplitude was  $3 V_0$  (d) The excitation efficiencies of the ions at different frequencies when the excitation period was 5ms and the excitation amplitude was  $0.2 V_0$

**The SWIFTSIN waveform isolation.** Inspired by the above observations, the SWIFTSIN waveform was designed for the high-resolution isolation of the target ion. The sample was a mixture of promethazine hydrochloride (labeled as B at 317 m/z), rotonidine (labeled as C and at 356 m/z), rosiglitazone (labeled as D at 358 m/z) and repaglinide (labeled as E, at 453 m/z). All the samples were diluted in methanol to final concentrations of 1mg/L. The injection period was 150ms, the frequency of the auxiliary AC signal was 230 kHz, and the amplitude was  $0.7 V_0$ . The full scan spectrum was shown in Figure 5a. It can be seen from the peaks of C and D that the spectral resolving power was poor without isolation. The SWIFT waveform with a notch from 227 kHz to 231 kHz and  $2.5 V_0$  was designed to roughly isolate rotonidine and rosiglitazone, and the resolution was significantly improved (inside Figure. 5a). In addition to the C isotope peak and the D isotope peak, the isotope peaks of C + 1, D + 1 and D + 2 were also included.

The SWIFTSIN waveform was designed for the high-resolution isolation of the target ion. High-resolution isolation corresponds to high-resolution excitation. In the first experiment, the notch band of the SWIFTSIN waveform was designed as 227 kHz to 231 kHz, with an amplitude of  $2.5 V_0$  in the time domain. The frequency of the superposed sinusoidal waveform was 229.2 kHz, and the amplitude was  $0.27 V_0$ . The SWIFT waveform was used to coarsely isolate rotonidine and rosiglitazone, and the sinusoidal waveform was used for the excitation of the C + 1 isotope ion. The SWIFT waveform was compressed to the first 15 ms of the whole period, and the sinusoidal waveform with a length of 5 ms was superposed on the latter half of the SWIFT waveform to achieve the purpose of coarse isolation to fine isolation. Figure 5b plots the isolation ability of the SWIFTSIN waveform. It can be seen that the C + 1 isotopic ion was excited, but the intensity of adjacent ions was not affected. The inner side of Figure 5b showed the isolation effect for a larger mass range, and you could see that B and E were effectively excited using the previous SWIFT waveform. Figure 5c shows the ability to isolate the D isotope ion using the SWIFTSIN waveform. In the design of the SWIFTSIN waveform, the notch of the SWIFT waveform was still designed to be 227 kHz to 231 kHz, but the difference was the superposition of four sinusoidal waveforms. The frequencies of the sinusoidal waveforms were 230 kHz, 229.2 kHz, 227.8 kHz, and 227.2 kHz, and the amplitudes were  $0.23 V_0$ ,  $0.12 V_0$ ,  $0.12 V_0$ , and  $0.23 V_0$ , respectively. They were used to excite isotope ions C, C + 1, D + 1, and D + 2, respectively. The red dashed line in Figure 5c shows that the D isotope ion is isolated without any loss of intensity. We also added collision-induced dissociation experiments to further prove that only the D isotope ion was isolated. The auxiliary AC signal for collision-induced dissociation was 50 kHz, and its amplitude was  $0.14V_0$ . The period was 100ms, and the RF voltage was  $195 V_0$  to  $205 V_0$ . Firstly, the ions after rough isolation were fragmented. Fig. 5d plots the secondary mass spectrum, where the isotope ion at m/z 135 corresponded to the fragment ion of rosiglitazone, and the isotope ions at m/z 165 and m/z 192 corresponded to the fragment ions of rotundine.<sup>40-43</sup> In addition, the isotope ion at m/z 136 also appeared (inside Figure 5e), according to the fragmentation law, which can be considered that the ion was the fragmentation of the rosiglitazone isotope. The D isotope ion obtained after fine isolation was fragmented, as in the interior of Figure 5e, only the fragment peak was retained at m/z 135

and other fragment peaks disappeared. It can be considered that the isolation of the D isotope ion was completed. From the primary and secondary mass spectrum, it can be seen that the intensity of the D isotope ion was not reduced after isolation, which is achieved at the expense of the isolation efficiency of some adjacent ions. As shown in Figure 5b, the intensity of the C + 1 isotope ion was not zero, but it retained a part of the intensity. However, compared with the SWIFT waveform, although it retained part of the intensity of some ions adjacent to the target ion, the isolation of the target ion still brought intensity loss, up to 30%, and combined with the previous excitation frequency bandwidths overlap theory, it is obvious that the SWIFTSIN has obvious advantages. Especially in Figure 5d and Figure 5e, it can be seen that although the intensity of the C + 1 isotope ion and the D + 1 isotope ion may still be retained in a small part, this small part was not been reflected in the secondary spectrum.

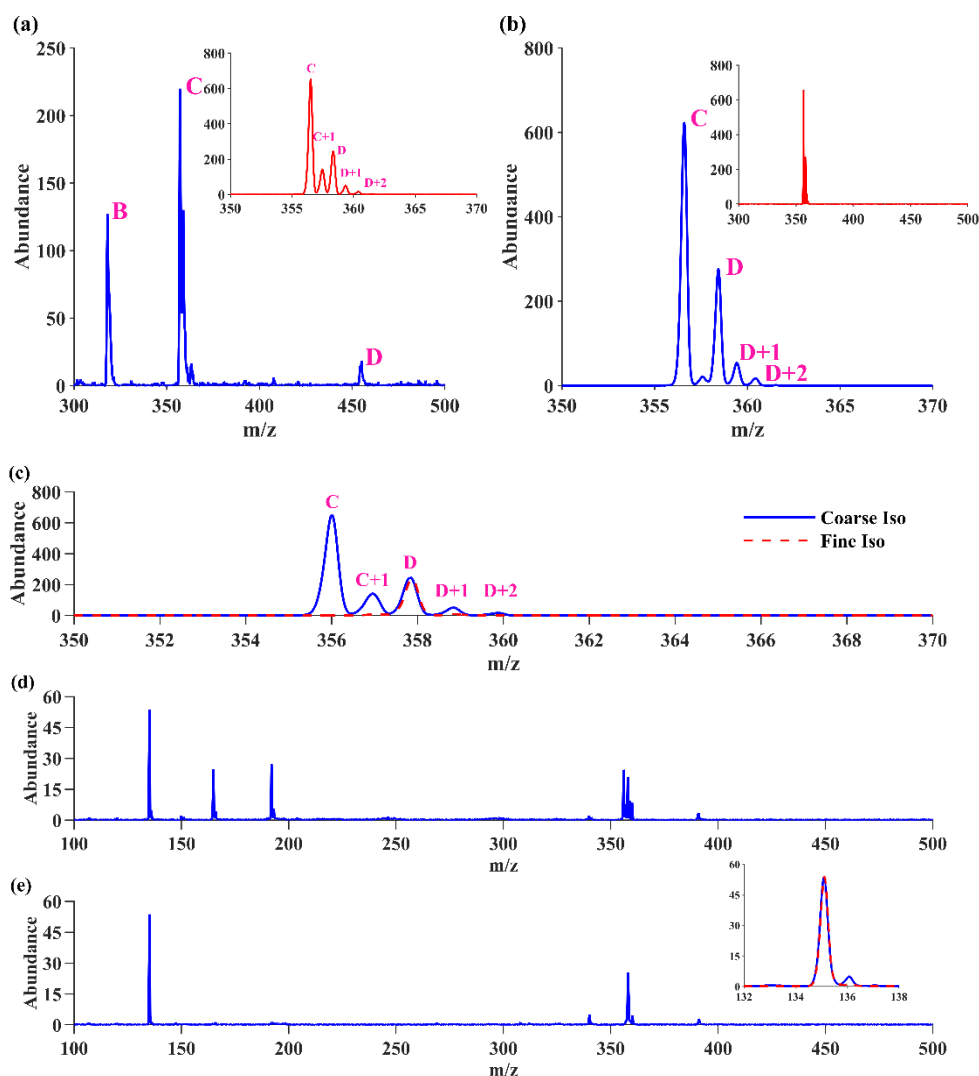


**Figure 5.** Isolation results using the SWIFTSIN waveform. The sample was a mixture of dioxypromazine hydrochloride, rotundine, rosiglitazone, and repaglinide, All samples were diluted in methanol to final concentrations of ~1mg/L, and the injection time was 150ms (a)

Full scan spectrum (b) Mass spectrum after the isotope ions B, C+1, and E were been excited, The inner side shows the spectrum of the larger mass range (c) Mass spectrum after the D isotope ion was isolated (d) Secondary mass spectrum after coarse isolation (e) Secondary spectrum after the D isotope ion was been isolated.

It is worth noting that when we designed the SWIFTSIN waveform, we used the most direct method to overlay a sinusoidal waveform onto the SWIFT waveform. The period of the sinusoidal waveform was 5ms. From the perspective of signal processing, the shorter the time is, the worse the resolution of the signal is. Therefore, the Gibbs effect could be observed in the notch of the amplitude spectrum of the SWIFTSIN waveform. However, when we used this direct superposition method to isolate the target ion, we did not find that the adjacent energy had any adverse effect on the target ion. Therefore, the isolation was completed by directly adding sinusoidal signals to the latter half of the isolated waveform.

## Conclusion

In this paper, the efficiencies of ion excitation under different excitation conditions were explored, and the idea of effective excitation frequency bandwidth was proposed. With special attention to the overlap of effective excitation frequency bandwidths of the adjacent ions, the reason for the lack of the high-resolution ion isolation ability of the SWIFT waveform was analyzed. On this basis, a simple yet efficient isolation waveform, the SWIFTSIN operating in a coarse-to-fine manner, was proposed. Using this waveform, the unit mass isolation was realized on the miniaturized ion trap mass spectrometer without reducing the intensity of the target ion. It is expected to further achieve better isolation under the condition of the higher performance of the instrument (such as allowing higher RF voltage). The high-resolution isolation can simplify MS/MS mass spectrum, helps to improve the on-site detection efficiency of miniaturized mass spectrometry, and also helps researchers further understand the cracking pathway of compounds. This isolation technology is not only suitable for small-scale mass spectrometry, but also for any type of ion trap mass spectrometry. It puts forward a solution to improve the performance of mass spectrometers, especially the ion trap mass spectrometry whose physical structure has been determined.

## Acknowledgement

This work was supported by National Natural Science Foundation of China (No. 22004079) and Shenzhen Natural Science Foundation (No. JCYJ20200109142824889)

## References

1. Liu, H.; Yao, G.; Liu, X.; Liu, C.; Zhan, J.; Liu, D.; Wang, P.; Zhou, Z., Approach for Pesticide Residue Analysis for Metabolite Prothioconazole-desthio in Animal Origin Food. *J Agric Food Chem* **2017**, *65* (11), 2481-2487.
2. Khrushcheva, M. L.; Krivosheina, M. S.; Matveeva, M. D.; Zhilyaev, D. I.; Borisov, R. S., New Matrix Compounds for the Detection of Carboxyl-Containing Nonsteroidal Anti-Inflammatory Drugs by MALDI Mass Spectrometry. *Russian Journal of Applied Chemistry* **2020**, *93* (8), 1244-1253.

3. Scholl, P. F.; Gray, P. J.; Harp, B. P.; Delmonte, P., High resolution mass spectral data from the analysis of copper chlorophylls and copper chlorophyll degradation products in bright green table olives. *Data Brief* **2020**, *30*, 105548.
4. Gonsalves, M. D.; Yevdokimov, A.; Brown-Nash, A.; Smith, J. L.; Oxley, J. C., Paper spray ionization-high-resolution mass spectrometry (PSI-HRMS) of peroxide explosives in biological matrices. *Anal Bioanal Chem* **2021**, *413* (11), 3069-3079.
5. Snyder, D. T.; Pulliam, C. J.; Ouyang, Z.; Cooks, R. G., Miniature and Fieldable Mass Spectrometers: Recent Advances. *Anal Chem* **2016**, *88* (1), 2-29.
6. Wang, X.; Zhou, X.; Ouyang, Z., Direct Analysis of Nonvolatile Chemical Compounds on Surfaces Using a Hand-Held Mass Spectrometer with Synchronized Discharge Ionization Function. *Anal Chem* **2016**, *88* (1), 826-31.
7. Li, G.; Li, D.; Cheng, Y.; Pei, X.; Zhang, H.; Wang, Y.; Sun, J.; Dong, M., Development of a low power miniature linear ion trap mass spectrometer with extended mass range. *Rev Sci Instrum* **2017**, *88* (12), 123108.
8. Pandey, S.; Hu, Y.; Bushman, L. R.; Castillo-Mancilla, J.; Anderson, P. L.; Cooks, R. G., Miniature mass spectrometer-based point-of-care assay for cabotegravir and rilpivirine in whole blood. *Anal Bioanal Chem* **2022**, *414* (11), 3387-3395.
9. Williams, J. D.; Cooks, R. G., REDUCTION OF SPACE-CHARGING IN THE QUADRUPOLE ION-TRAP BY SEQUENTIAL INJECTION AND SIMULTANEOUS STORAGE OF POSITIVELY AND NEGATIVELY CHARGED IONS. *RAPID COMMUNICATIONS IN MASS SPECTROMETRY* **1993**, *7* (5), 380-382.
10. Tian, Y.; Higgs, J.; Li, A.; Barney, B.; Austin, D. E., How far can ion trap miniaturization go? Parameter scaling and space-charge limits for very small cylindrical ion traps. *J Mass Spectrom* **2014**, *49* (3), 233-40.
11. Jiang, T.; Xu, Q.; Zhang, H. J.; Li, D. Y.; Xu, W., Improving the Performances of a "Brick Mass Spectrometer" by Quadrupole Enhanced Dipolar Resonance Ejection from the Linear Ion Trap. *ANALYTICAL CHEMISTRY* **2018**, *90* (19), 11671-11679.
12. Mielczarek, P.; Silberring, J.; Smoluch, M., Miniaturization in Mass Spectrometry. *Mass Spectrom Rev* **2020**, *39* (5-6), 453-470.
13. Acosta-Martin, A. E.; Coelho Graca, D.; Antinori, P.; Clerici, L.; Hartmer, R.; Meyer, M.; Hochstrasser, D.; Samii, K.; Lescuyer, P.; Scherl, A., Quantitative mass spectrometry analysis of intact hemoglobin A2 by precursor ion isolation and detection. *Anal Chem* **2013**, *85* (16), 7971-5.
14. Xu, Z.; Jiang, T.; Xu, Q.; Zhai, Y.; Li, D.; Xu, W., Pseudo-Multiple Reaction Monitoring (Pseudo-MRM) Mode on the "Brick" Mass Spectrometer, Using the Grid-SWIFT Waveform. *Anal Chem* **2019**, *91* (21), 13838-13846.
15. Barr, J. M.; Van Stipdonk, M. J., Multi-stage tandem mass spectrometry of metal cationized leucine enkephalin and leucine enkephalin amide. *Rapid Commun Mass Spectrom* **2002**, *16* (6), 566-78.
16. Cousins, L. M.; Thomson, B. A., MS3 using the collision cell of a tandem mass spectrometer system. *Rapid Commun Mass Spectrom* **2002**, *16* (11), 1023-34.
17. Naoki; Tanaka; Keiko; Nagasaka; Yasuhiko; Komatsu, Selected reaction monitoring by linear ion-trap mass spectrometry can effectively be applicable to simultaneous quantification of multiple peptides. *Biological & Pharmaceutical Bulletin* **2011**.

18. Schwartz, J. C.; Jaardine, I., High resolution parent-ion selection/isolation using a quadrupole ion-trap mass spectrometer. *Rapid Communications in Mass Spectrometry* **1992**, *6* (4), 313-317.
19. Snyder, D. T.; Cooks, R. G., Ion isolation and multigenerational collision-induced dissociation using the inverse Mathieu q scan. *RAPID COMMUNICATIONS IN MASS SPECTROMETRY* **2017**, *31* (2), 200-206.
20. Wang, W.; Dong, M.; Song, C.; Cai, X.; Liu, Y.; Liu, Z.; Tian, S., Structural information of asphaltenes derived from petroleum vacuum residue and its hydrotreated product obtained by FT-ICR mass spectrometry with narrow ion isolation windows. *Fuel* **2018**, *227*, 111-117.
21. Cataldi, T. R. I.; Lelario, F.; Orlando, D.; Bufo, S. A., Collision-Induced Dissociation of the A + 2 Isotope Ion Facilitates Glucosinolates Structure Elucidation by Electrospray Ionization-Tandem Mass Spectrometry with a Linear Quadrupole Ion Trap. *Analytical Chemistry* **2010**, *82* (13), 5686-5696.
22. Bianco, G.; Buchicchio, A.; Lelario, F.; Cataldi, T. R., Molecular formula analysis of fragment ions by isotope-selective collision-induced dissociation tandem mass spectrometry of pharmacologically active compounds. *J Mass Spectrom* **2014**, *49* (12), 1322-9.
23. He, L.; Wu, J.-T.; Parus, S.; Lubman, D. M., Development of a capillary high-performance liquid chromatography tandem mass spectrometry system using SWIFT technology in an ion trap/reflectron time-of-flight mass spectrometer. *Rapid Communications in Mass Spectrometry* **1997**, *11* (16), 1739-1748.
24. Murrell, J.; Konn, D. O.; Underwood, N. J.; Despeyroux, D., Studies into the selective accumulation of multiply charged protein ions in a quadrupole ion trap mass spectrometer. *International Journal of Mass Spectrometry* **2003**, *227* (2), 223-234.
25. Ruddy, B. M.; Blakney, G. T.; Rodgers, R. P.; Hendrickson, C. L.; Marshall, A. G., Elemental composition validation from stored waveform inverse Fourier transform (SWIFT) isolation FT-ICR MS isotopic fine structure. *J Am Soc Mass Spectrom* **2013**, *24* (10), 1608-11.
26. Ruddy; Mark, B., Investigation of Deepwater Horizon Heavy End Environmental Transformation by High Resolution Detection and Isolation Fourier Transform Ion Cyclotron Resonance Mass Spectrometry. **2016**.
27. Smith, D. F.; Blakney, G. T.; Beu, S. C.; Anderson, L. C.; Weisbrod, C. R.; Hendrickson, C. L., Ultrahigh Resolution Ion Isolation by Stored Waveform Inverse Fourier Transform 21 T Fourier Transform Ion Cyclotron Resonance Mass Spectrometry. *Anal Chem* **2020**, *92* (4), 3213-3219.
28. Kenny, D. V.; Callahan, P. J.; Gordon, S. M.; Stiller, S. W., SIMULTANEOUS ISOLATION OF 2 DIFFERENT M/Z IONS IN AN ION-TRAP MASS-SPECTROMETER AND THEIR TANDEM MASS-SPECTRA USING FILTERED-NOISE FIELDS. *RAPID COMMUNICATIONS IN MASS SPECTROMETRY* **1993**, *7* (12), 1086-1089.
29. Goeringer, D. E.; Asano, K. G.; McLuckey, S. A.; Hoekman, D.; Stiller, S. W., FILTERED NOISE FIELD SIGNALS FOR MASS-SELECTIVE ACCUMULATION OF EXTERNALLY FORMED IONS IN A QUADRUPOLE ION-TRAP. *ANALYTICAL CHEMISTRY* **1994**, *66* (3), 313-318.
30. Hilger, R. T.; Santini, R. E.; Luongo, C. A.; Prentice, B. M.; McLuckey, S. A., A method for isolating ions in quadrupole ion traps using an excitation waveform generated by frequency modulation and mixing. *INTERNATIONAL JOURNAL OF MASS SPECTROMETRY* **2015**, *377*, 329-337.

31. Sun, J.; Yan, H.; Li, D. In *A Method for Isolating Ions Using an Excitation Signal Generated by Superposing and Modulation Frequency*, 2019 12th International Congress on Image and Signal Processing, BioMedical Engineering and Informatics (CISP-BMED), 19-21 Oct. 2019; 2019; pp 1-5.
32. Guan, S. H., GENERAL PHASE MODULATION METHOD FOR STORED WAVEFORM INVERSE FOURIER-TRANSFORM EXCITATION FOR FOURIER-TRANSFORM ION-CYCLOTRON RESONANCE MASS-SPECTROMETRY. *JOURNAL OF CHEMICAL PHYSICS* **1989**, *91* (2), 775-777.
33. Guan, S., Optimal phase modulation in stored waveform inverse Fourier transform excitation for Fourier transform mass spectrometry. II. Magnitude spectrum smoothing. *The Journal of Chemical Physics* **1990**, *93* (12), 8442-8445.
34. Guan, S. H.; Marshall, A. G., Stored waveform inverse Fourier transform (SWIFT) ion excitation in trapped-ion mass spectrometry: Theory and applications. *INTERNATIONAL JOURNAL OF MASS SPECTROMETRY* **1996**, *157*, 5-37.
35. Soni, M. H.; Cooks, R. G., SELECTIVE INJECTION AND ISOLATION OF IONS IN QUADRUPOLE ION-TRAP MASS-SPECTROMETRY USING NOTCHED WAVE-FORMS CREATED USING THE INVERSE FOURIER-TRANSFORM. *ANALYTICAL CHEMISTRY* **1994**, *66* (15), 2488-2496.
36. Doroshenko, V. M.; Cotter, R. J., Advanced stored waveform inverse Fourier transform technique for a matrix-assisted laser desorption/ionization quadrupole ion trap mass spectrometer. *RAPID COMMUNICATIONS IN MASS SPECTROMETRY* **1996**, *10* (1), 65-73.
37. Zhang, X.; Huo, X.; Tang, F.; Zha, Z.; Yang, F.; Ni, Y.; Wang, Y.; Zhou, M.; Wang, X., Characterisation and optimisation of ion discrimination in a mini ion funnel for a miniature mass spectrometer. *Analytical methods* **2019**.
38. Huo, X.; Zhu, X.; Tang, F.; Zhang, J.; Zhang, X.; Yu, Q.; Wang, X., Discontinuous Subatmospheric Pressure Interface Reduces the Gas Flow Effects on Miniature CAPI Mass Spectrometer. *Analytical Chemistry* **2020**, *92* (5), 3707-3715.
39. Guan, S.; Jones, P. R., General phase modulation method for stored waveform inverse fourier transform excitation for fourier transform ion cyclotron resonance mass spectrometry. *Journal of Chemical Physics* **1989**, *91*, 775-777.
40. Chou, C. C.; Lee, M. R.; Cheng, F. C.; Yang, D. Y., Solid-phase extraction coupled with liquid chromatography-tandem mass spectrometry for determination of trace rosiglitazone in urine. *Journal of Chromatography A* **2005**, *1097* (1-2), 74-83.
41. Xiao-mei, Z.; Qing-hui, L. I. N.; Chun-zheng, L. I.; Jing-ting, D.; Hua, L. I., In vitro comparison of rotundine metabolism in liver microsomes of human,dog and rat. *Chinese Pharmacological Bulletin* **2009**, *25* (9), 1147-1152.
42. Yu, F. F.; Lv, H. N.; Dong, W. J.; Ye, J.; Hao, H. Z.; Ma, S. G.; Yu, S. S.; Liu, Y. L., Development and validation of a liquid chromatography-tandem mass spectroscopy method for simultaneous determination of (+)-(13aS)-deoxytylophorinine and its pharmacologically active 3-O-desmethyl metabolite in rat plasma. *Journal of Pharmaceutical and Biomedical Analysis* **2015**, *107*, 223-228.
43. Rashid, J.; Ahsan, F., A highly sensitive LC-MS/MS method for concurrent determination of sildenafil and rosiglitazone in rat plasma. *Journal of Pharmaceutical and Biomedical Analysis* **2016**, *129*, 21-27.